

*Research Article*

# Determination of Fe<sup>3+</sup> in Water Samples by Reduced Schiff Base Ligand

Sunti DOUNGCHANDENG<sup>1</sup>, Nuttapon APIRATIKUL<sup>1</sup>, Itthipol SUNGWIEWONG<sup>1</sup>,  
Piyarat SRIVILAI<sup>1</sup> and Pan TONGRAUNG<sup>1\*</sup>

---

*Received: 14 November 2024*

*Revised: 7 December 2024*

*Accepted: 12 December 2024*

## ABSTRACT

This research presents the development of a method for the quantification of Fe<sup>3+</sup> using a reduced Schiff base ligand, which was synthesized via a simple two-step process with a high yield of 84%. The quantification of Fe<sup>3+</sup> was analyzed using UV-Visible spectrophotometry. The selective binding of ligand with various cations (Fe<sup>3+</sup>, Cr<sup>3+</sup>, Pb<sup>2+</sup>, Co<sup>2+</sup>, Cu<sup>2+</sup>, Zn<sup>2+</sup>, Cd<sup>2+</sup>, Hg<sup>2+</sup>, Mn<sup>2+</sup>, Ni<sup>2+</sup>, Fe<sup>2+</sup>, Mg<sup>2+</sup>, Ag<sup>+</sup>, Na<sup>+</sup>, K<sup>+</sup>) was investigated. The results revealed that the reduced Schiff base ligand specifically formed a complex with Fe<sup>3+</sup>, indicated by a new absorption peak in the 350–400 nm range due to ligand-to-metal charge transfer (LMCT). In contrast, other cations induced no significant spectral changes. Quantitative studies of Fe<sup>3+</sup> showed that the absorbance at 380 nm increased linearly with Fe<sup>3+</sup> concentration, displaying a correlation coefficient (R<sup>2</sup>) of 0.9994 within the Fe<sup>3+</sup> concentration range of 2.00 × 10<sup>-6</sup> to 1.00 × 10<sup>-3</sup> M. The method exhibited a limit of detection (LOD) of 1.22 × 10<sup>-6</sup> M and a limit of quantification (LOQ) of 2.03 × 10<sup>-5</sup> M. The reduced Schiff base ligand was successfully applied for Fe<sup>3+</sup> quantification in real water samples, corresponding to the results obtained by inductively coupled plasma optical emission spectroscopy (ICP-OES).

**Keywords:** Reduced Schiff base ligand, Sensor, Fe<sup>3+</sup>, Water samples.

---

<sup>1</sup> Department of Chemistry, Faculty of Science, Srinakharinwirot University, Bangkok 10110, Thailand

\*Corresponding author, email: pan@g.swu.ac.th

## Introduction

Iron is an important element in the human body. It is extremely important for the metabolic process which plays an important role in physiology. Iron displays a role in many chemical and biological processes, such as metabolic processes, oxygen transport respiration and electron transfer [1-4]. Quantification of iron is important for human health. Accumulation of iron in the body can result in kidney and liver damage, including abnormalities of vital organs which can cause cancer, hemochromatosis, and symptoms of hepatitis [5-8]. Iron deficiency prevents the synthesis of certain enzymes and proteins which can affect oxygen transport, causing many diseases, including cell metabolism problems and anemia [9-11]. The average amount of iron that a person should receive is approximately 3.8 grams for men and 2.3 grams for women [12-13].

Water is an essential resource for all living organisms, especially humans. Wastewater from industrial factories lacking effective waste control and treatment systems, as well as from agriculture and household activities, often flows into water sources, contaminating them with heavy metals. Iron is one of metals that contaminates water sources, causing in water pollution. Therefore, monitoring and assessing the quality of water resources, including iron content, is critically important.

From the importance of iron mentioned above, accurate analysis of iron content in various samples, especially water samples, is therefore very important. Numerous methods have been developed for iron analysis in many samples [14-19]. There are several techniques that can be used to analyzed iron with high sensitivity, good accuracy and precision. However, these techniques are usually large and expensive, and require an analytical person with experience and expertise in using tools. Moreover, some techniques require complicated sample preparation before analysis.

Over the past decades, many researchers have been interested in designing and synthesizing chemosensors to simply measure heavy metals with good specificity and high sensitivity. Schiff base groups are frequently incorporated into chemosensor designs due to their unique properties; 1) being both a receiver and a transmitter, 2) various precursors for synthesis and easy to find, and 3) easy to synthesize and purify with high productivity and low costs [20-23]. Schiff base can bind to metal ions including iron ions and change the optical signal. Researchers are therefore competing to design synthetic chemosensors that can detect heavy metals with a low LOD and a wide measurement range [24] with high efficiency [25]. Although these chemosensors have various advantages mentioned above, but they do not selectively bind to only one type of metal ion. They rather bind with more than one type of metal ion [25-28].

Longyan Wang et al. [11] reported a Schiff base probe obtained by the synthesis of diketopyrrolopyrrole and *p*-methoxyaniline which can be used to measure  $\text{Fe}^{3+}$  and  $\text{Al}^{3+}$  with decreased fluorescence signal when binding to  $\text{Fe}^{3+}$  and increased signal when binding to  $\text{Al}^{3+}$ . Min Zhang et al. [29] reported a Schiff base probe, synthesized from 2-hydroxy-1-naphthaldehyde and 5-aminosalicylic acid, that can measure  $\text{Fe}^{3+}$ ,  $\text{Al}^{3+}$ ,  $\text{Cr}^{3+}$ , and  $\text{Cu}^{2+}$ . There was an increase in the fluorescent signal when binding with  $\text{Al}^{3+}$ , and a decrease in the fluorescent signal when binding with  $\text{Fe}^{3+}$ . Changes of color of the solution were observed differently when binding with  $\text{Cr}^{3+}$  and  $\text{Cu}^{2+}$ .

The synthesis of chemosensors that selectively bind to  $\text{Fe}^{3+}$  by altering the fluorescent signal has been reported. However, there were many complicated synthesis steps that resulted in low yield. Most importantly, they used solvents that were not environmentally friendly [30-32]. Li, Z. et al. [33] synthesized

a chemosensor that selectively bound to  $\text{Fe}^{3+}$  in a 'turn on' manner with a four-step synthesis process using DMF and  $\text{CHCl}_3$  as solvents. Ruiping, W. et al. [34] also synthesized a chemosensor that specifically bound to  $\text{Fe}^{3+}$ , but pyridine was used as a solvent with 3 steps of synthesis, resulting in low yield. Changing the chemosensor to reduced Schiff base ligand allowed it to selectively bind to  $\text{Fe}^{3+}$ . It has been reported that synthesized Schiff base - naphthalene-2-ol [35] can selectively bind to  $\text{Cu}^{2+}$ , but when reducing Schiff base was made, it was found that it could selectively bind to only  $\text{Fe}^{3+}$ . Importantly, the synthesis was easy with high yield. When binding to  $\text{Fe}^{3+}$ , the fluorescent signal was suppressed, and spectral changes occurred due to electron transfer from ligand to metal ion (LMCT). In addition, this research group performed a preliminary  $\text{Fe}^{3+}$  binding study with the fluorescence signal decreasing with addition of  $\text{Fe}^{3+}$  [36]. However, reduced Schiff base has not been used as a detector to quantify  $\text{Fe}^{3+}$  in real samples.

Given the critical role of  $\text{Fe}^{3+}$  in biological and environmental systems, accurate  $\text{Fe}^{3+}$  quantification is essential for water quality assessment. Therefore, this research is interested in using reduced Schiff base ligand with simple synthesis and high yield. The specificity of this reduced Schiff base ligand as a sensor to determine the amount of  $\text{Fe}^{3+}$  in water samples with low lower limit of detection (LOD) and a linear coefficient ( $R^2$ ) close to 1, make it a viable alternative for  $\text{Fe}^{3+}$  quantification in real water samples.

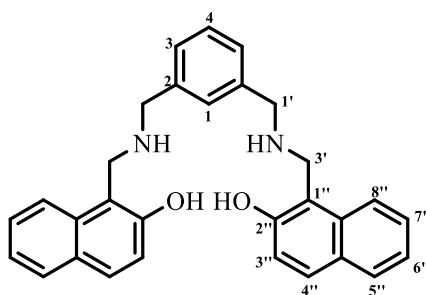


**Figure 1** Structure of reduced Schiff base (RSB).

## Materials and Methods

### Chemicals and Equipment

A UV-visible spectrophotometer (model UV-2401PC, Shimadzu) was used to record absorption spectra and to measure absorbance. A nuclear magnetic resonance spectrometer (model Bruker Ascend 500, Bruker) was used at 500 MHz for  $^1\text{H}$ -NMR, and at 125 MHz for  $^{13}\text{C}$ -NMR. A mass spectrometer (model Dal-tonics (micro TOF), Bruker) was used to record mass spectra. Inductively coupled plasma optical emission spectroscopy (Perkin Elmer Avio 200) was used as a reference technique to compare the iron(III) content analysis results in the samples.

Salts of various types of heavy metal ions including  $\text{Cd}(\text{ClO}_4)_2 \cdot \text{H}_2\text{O}$  (99.9%),  $\text{Cu}(\text{ClO}_4)_2 \cdot 6\text{H}_2\text{O}$  (98%),  $\text{Fe}(\text{ClO}_4)_2 \cdot \text{H}_2\text{O}$  (98%),  $\text{Fe}(\text{ClO}_4)_3 \cdot \text{H}_2\text{O}$ ,  $\text{Ni}(\text{ClO}_4)_2 \cdot 6\text{H}_2\text{O}$  (98%),  $\text{Mn}(\text{ClO}_4)_2 \cdot 6\text{H}_2\text{O}$  (99%),  $\text{Pb}(\text{ClO}_4)_2 \cdot 3\text{H}_2\text{O}$  (99%),  $\text{Zn}(\text{ClO}_4)_2 \cdot 6\text{H}_2\text{O}$  (98%),  $\text{AgNO}_3$  (99%), and  $\text{HgCl}_2$  (98%) were purchased from Sigma Aldrich.  $\text{NaCl}$  (98%),  $\text{KCl}$  (98%),  $\text{MgCl}_2$  (98%), and  $\text{CrCl}_3 \cdot 6\text{H}_2\text{O}$  (95%) were purchased from UNILAB. All chemicals were AR grade.

### ***Synthesis of reduced Schiff base***

The synthesis of reduced Schiff base ligand has been reported from the research of Sungwienwong et al. [36], which is a simple synthesis method, using a mild reaction with high yield (84%). The structure of reduced Schiff base ligand was characterized by IR,  $^1\text{H-NMR}$ ,  $^{13}\text{C-NMR}$  and mass spectrometry. The results are as following: IR (ATR)  $\nu_{\text{max}}$  3293, 3055, 2851, 1621, 1597, 1514, 1467, 1437, 1357, 1327, 1267, 1235, 1130, 1089, 955, 904, 812, 744  $\text{cm}^{-1}$ ;  $^1\text{H-NMR}$  (500 MHz, DMSO  $d_6$ ):  $\delta$  3.63 (4H, s, H-3'), 4.01 (4H, s, H-1'), 7.07 (2H, d,  $J = 8.8$  Hz, H-3''), 7.10 (2H, t,  $J = 7.6$  Hz, H-7''), 7.17–7.21 (5H, m, H-1, H-3, H-6''), 7.35 (1H, t,  $J = 7.4$  Hz, H-4), 7.59 (2H, d,  $J = 8.5$  Hz, H-8''), 7.65 (2H, d,  $J = 8.8$  Hz, H-4''), 7.70 (2H, d,  $J = 8.0$  Hz, H-5'');  $^{13}\text{C-NMR}$  (125 MHz, DMSO  $d_6$ ):  $\delta$  48.1 (C-1'), 58.1 (C-3'), 113.8 (C-9''), 118.0 (C-3''), 122.3 (C-6''), 122.7 (C-8''), 125.8 (C-7''), 128.0 (C-10''), 128.1 (C-5''), 128.6 (C-3), 129.0 (C-4''), 131.3 (C-1), 133.4 (C-1''), 137.7 (C-2), 154.5 (C-2''); HR-ESI-MS  $m/z$  449.2231  $[\text{M} + \text{H}]^+$  (calculated for  $\text{C}_{30}\text{H}_{29}\text{N}_2\text{O}_2$  449.2223).

### ***Study of the selective binding of reduced Schiff base ligand with various cations.***

The solutions of metal cations;  $\text{Na}^+$ ,  $\text{K}^+$ ,  $\text{Mg}^{2+}$ ,  $\text{Mn}^{2+}$ ,  $\text{Fe}^{2+}$ ,  $\text{Co}^{2+}$ ,  $\text{Ni}^{2+}$ ,  $\text{Cu}^{2+}$ ,  $\text{Zn}^{2+}$ ,  $\text{Hg}^{2+}$ ,  $\text{Cd}^{2+}$ ,  $\text{Pb}^{2+}$ ,  $\text{Cr}^{3+}$ ,  $\text{Fe}^{3+}$  ( $3.00 \times 10^{-4}$  M) and the solution of reduced Schiff base ( $1.00 \times 10^{-5}$  M) were prepared. The reduced Schiff base solution (2.00 mL) was mixed with each metal ion (2.00 mL). The absorbance of the mixtures was determined at 250–700 nm.

The solutions of metal cations;  $\text{Na}^+$ ,  $\text{K}^+$ ,  $\text{Mg}^{2+}$ ,  $\text{Mn}^{2+}$ ,  $\text{Fe}^{2+}$ ,  $\text{Co}^{2+}$ ,  $\text{Ni}^{2+}$ ,  $\text{Cu}^{2+}$ ,  $\text{Zn}^{2+}$ ,  $\text{Hg}^{2+}$ ,  $\text{Cd}^{2+}$ ,  $\text{Pb}^{2+}$ ,  $\text{Cr}^{3+}$ ,  $\text{Fe}^{3+}$  ( $1.00 \times 10^{-4}$  M) and the solution of reduced Schiff base ( $1.00 \times 10^{-5}$  M) were prepared. The reduced Schiff base solution (1.00 mL) was mixed with each metal ion (1.00 mL). The absorbance of the mixtures was determined at 380 nm. Then, the solution of  $\text{Fe}^{3+}$  (1.00 mL) was added to the above mixture solution, and the absorbance of the solutions was determined at 380 nm. The absorbance in the absence and presence of  $\text{Fe}^{3+}$  was compared.

### ***Binding study of reduced Schiff base with $\text{Fe}^{3+}$***

The titration of reduced Schiff base ligand was performed by adding the  $\text{Fe}^{3+}$  solution ( $1.00 \times 10^{-3}$  M) 50  $\mu\text{L}$ -interval to the reduced Schiff base ligand ( $1.00 \times 10^{-5}$  M, 2.00 mL) until the volume of  $\text{Fe}^{3+}$  solution was 800  $\mu\text{L}$ . The absorption spectra were measured in the wavelength range of 300–700 nm, and the spectra of the reduced Schiff base ligand in the presence of each concentration of  $\text{Fe}^{3+}$  were compared.

The absorption spectra of standard  $\text{Fe}^{3+}$  solution with various concentrations,  $3.00 \times 10^{-6}$ ,  $1.00 \times 10^{-4}$ ,  $2.00 \times 10^{-4}$ ,  $3.00 \times 10^{-4}$ ,  $5.00 \times 10^{-4}$  and  $1.00 \times 10^{-3}$  M, were measured at 380 nm. Calibration curve of the absorbance versus standard  $\text{Fe}^{3+}$  concentration was constructed for LOD and LOQ determination.

### ***The effect of pH on $\text{Fe}^{3+}$ measurement with reduced Schiff base ligand.***

The reduced Schiff base ligand ( $1.00 \times 10^{-5}$  M) and  $\text{Fe}^{3+}$  ( $3.00 \times 10^{-4}$  M) solutions were prepared at pH 3, 5, 9 and 12. The absorbance at 380 nm of reduced Schiff base ligand solution (2.00 mL) was measured in the absence and presence of standard  $\text{Fe}^{3+}$  solution (2.00 mL) for all pHs.

### ***The interferent effect of various metal ions on Fe<sup>3+</sup> measurement with reduced Schiff base ligand***

The reduced Schiff base ligand ( $1.00 \times 10^{-5}$  M, 2.00 mL) was mixed with Fe<sup>3+</sup> solution ( $1.00 \times 10^{-4}$  M, 1.00 mL). The absorbance at 380 nm of the mixture solution was measured. Then, the absorbance was measured with addition of other metal ions ( $3.00 \times 10^{-4}$  M, 1.00 mL) to the above mixture.

### ***Application of reduced Schiff base for quantitation of Fe<sup>3+</sup> in water samples***

Water sample solutions with Fe<sup>3+</sup> concentrations of  $1.0 \times 10^{-4}$  M and  $3.00 \times 10^{-4}$  M in tap water, canal water, and drinking water were prepared by calculating the volume of Fe<sup>3+</sup> solution used from the standard solution. Then, the volume was adjusted with tap water, canal water and drinking water. The reduced Schiff base ligand solution ( $1.00 \times 10^{-5}$  M, 2.00 mL) was mixed with each type of water sample. The absorbance at a wavelength of 380 nm was measured, and used to determine the amount of Fe<sup>3+</sup> from the standard calibration curve.

## **Results and Discussion**

The synthesis of reduced Schiff base ligand has been reported in the research of Sungwienwong et al. [36] using the coupling reaction between 2-hydroxy-1-naphthadehyde and *m*-xylylene diamine to obtain Schiff base naphthalene-2-ol and reduced with sodium borohydride (NaBH<sub>4</sub>) to obtain reduced Schiff base. The structure of reduced Schiff base was identified using NMR, IR and mass spectroscopic techniques.

The specificity study of the reduced Schiff base ligand in selective binding to various types of metal ions, including Fe<sup>3+</sup>, Cr<sup>3+</sup>, Pb<sup>2+</sup>, Co<sup>2+</sup>, Cu<sup>2+</sup>, Zn<sup>2+</sup>, Cd<sup>2+</sup>, Hg<sup>2+</sup>, Mn<sup>2+</sup>, Ni<sup>2+</sup>, Ag<sup>+</sup>, Na<sup>+</sup>, Mg<sup>2+</sup>, K<sup>+</sup>, Fe<sup>2+</sup> showed only selectivity of Fe<sup>3+</sup>. New peaks in the range of 350-420 nm were observed with the significant change of the absorption spectrum of reduced Schiff base due to ligand-to-metal charge transfer (LMCT). However, other metal ions did not change the spectra of reduced Schiff base except Fe<sup>2+</sup> and Cu<sup>2+</sup>, as shown in Figure 2. The reduced Schiff base ligand showed selective binding to Fe<sup>3+</sup> as observed by the increase of the absorbance of reduced Schiff base ligand when Fe<sup>3+</sup> was added, as shown in Figure 3.

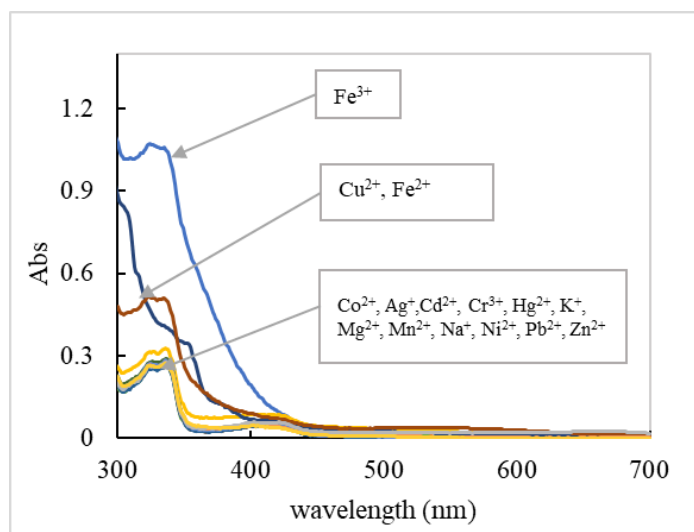


**Figure 2** Absorption spectra of reduced Schiff base solution in the presence of various metal ions ( $3.0 \times 10^{-4}$  M).

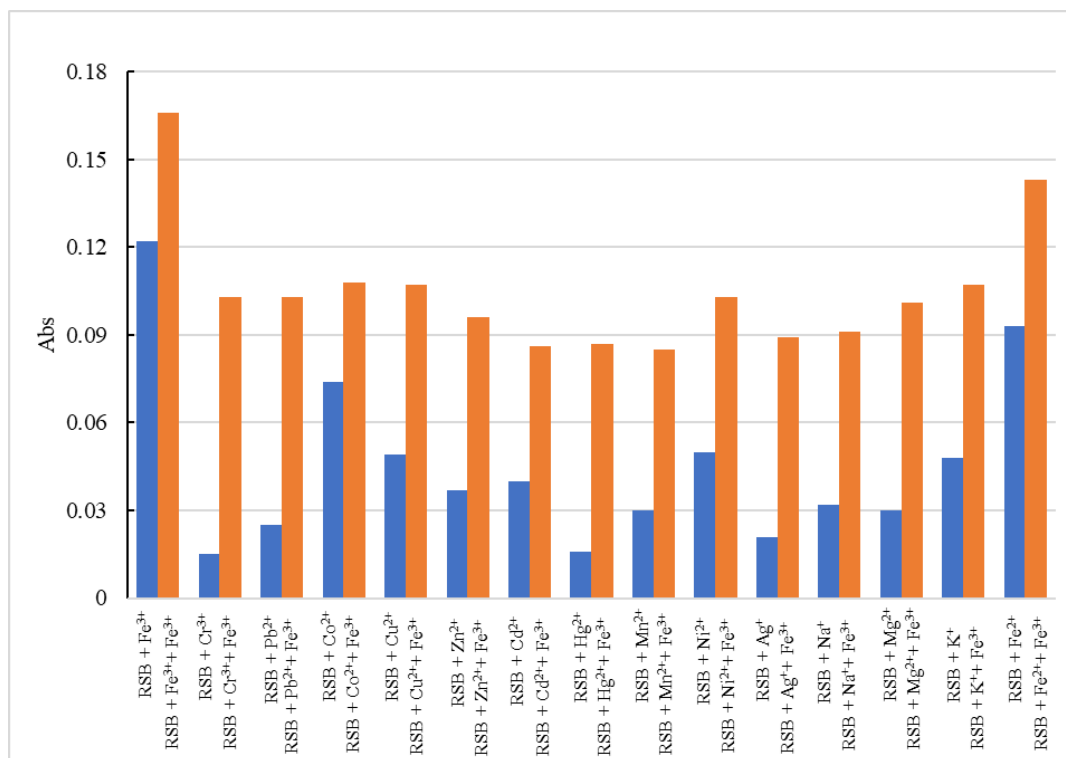


**Figure 3** The bar graph shows the absorbance of RSB ( $1.00 \times 10^{-5}$  M) with various metal ions ( $3.00 \times 10^{-4}$  M) before adding (blue) and after adding  $3.00 \times 10^{-4}$  M of  $Fe^{3+}$  solution (orange) at 380 nm.

The binding efficiency of the reduced Schiff base ligand with  $Fe^{3+}$  was evaluated by monitoring absorbance changes upon  $Fe^{3+}$  addition. When  $Fe^{3+}$  was added to the reduced Schiff base ligand solution, the absorbance in the wavelength range of 350-420 nm increased with increasing volume of  $Fe^{3+}$ , as shown in Figure 4. The plot of absorbance value at a wavelength of 380 nm versus the concentration of  $Fe^{3+}$  added gave a straight line with a linear correlation coefficient ( $R^2$ ) of 0.9974, as shown in Figure 5.

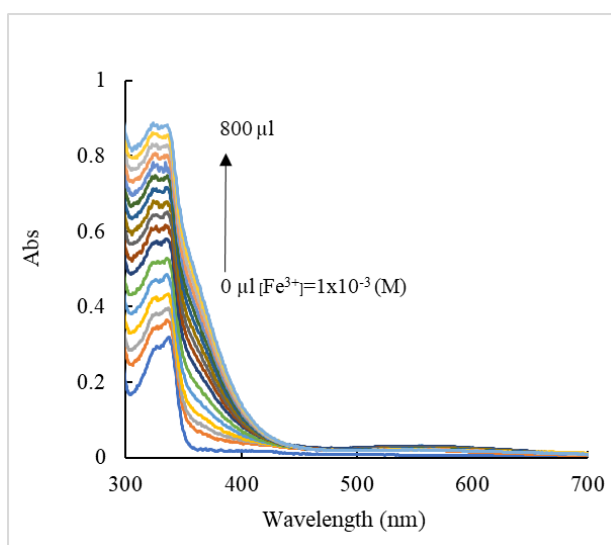


**Figure 4** Absorption spectra of reduced Schiff base solution in the presence of 0.0-800.0  $\mu$ L of  $1.0 \times 10^{-3}$  M  $Fe^{3+}$ .

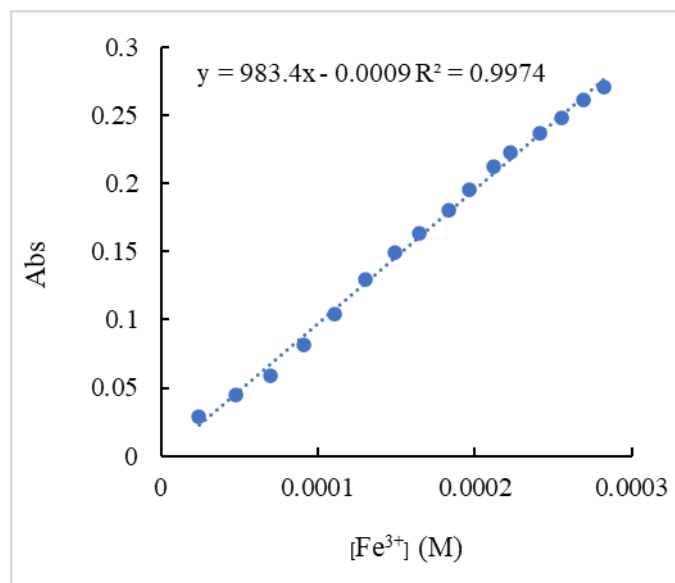


**Figure 5** The linear relationship of absorbance versus  $\text{Fe}^{3+}$  concentration.

The linear relationship of the absorbance at 380 nm with the  $\text{Fe}^{3+}$  concentration with a linear correlation coefficient ( $R^2$ ) of 0.9994 was confirmed by creating a standard curve. The limit of detection (LOD) and limit of quantification (LOQ) were calculated as three times and ten times the standard deviation (SD) of the blank solution signal measurements in 10 replicates. LOD and LOQ were found to be  $1.22 \times 10^{-6}$  M and  $2.03 \times 10^{-6}$  M, respectively, as shown in Figure 6.

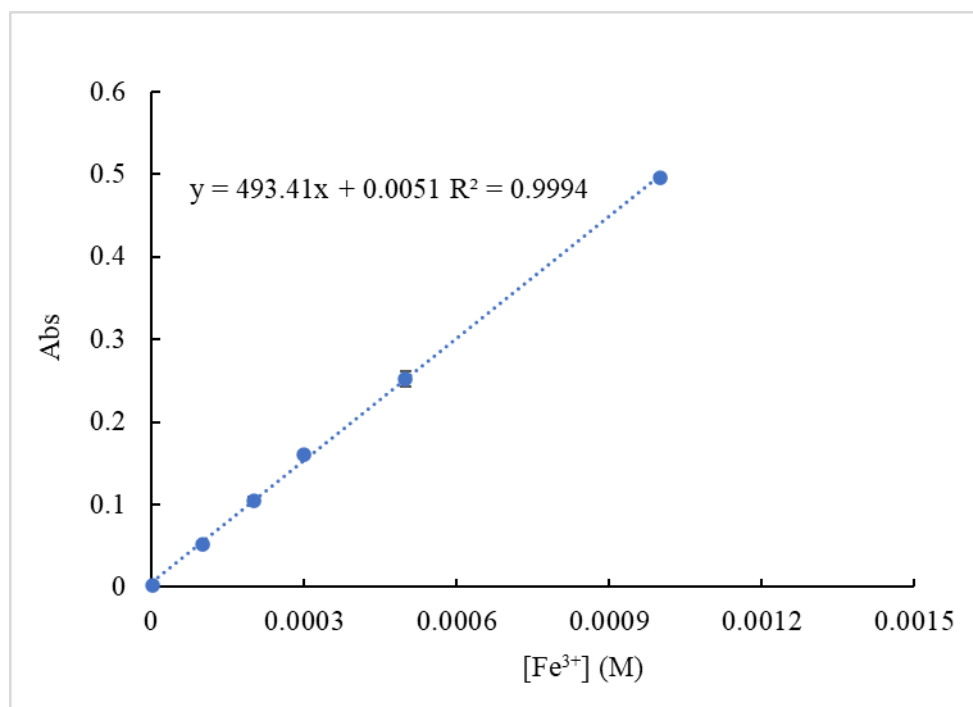


**Figure 6** Standard graph showing a linear relationship between the absorbance at 380 nm and  $\text{Fe}^{3+}$  concentration in the range of  $1.00 \times 10^{-6}$  -  $1.00 \times 10^{-3}$  M when using the reduced Schiff ligand at a concentration of  $1.00 \times 10^{-5}$  M.

The results of the pH effect on the reduced Schiff base ligand solution in the range pH of 3–12 are shown in Figure 7. The spectra of the reduced Schiff base ligand at pH 3–12 did not change. Only at pH 3, the absorbance at the highest wavelength decreased due to the protonation of OH and NH functional groups of RSB. Comparison the spectra of reduced Schiff base ligand solution at the pH 3–12 before and after adding  $Fe^{3+}$  throughout the studied pH range, showed no effect of pH on  $Fe^{3+}$  binding, as shown in Figure 8.

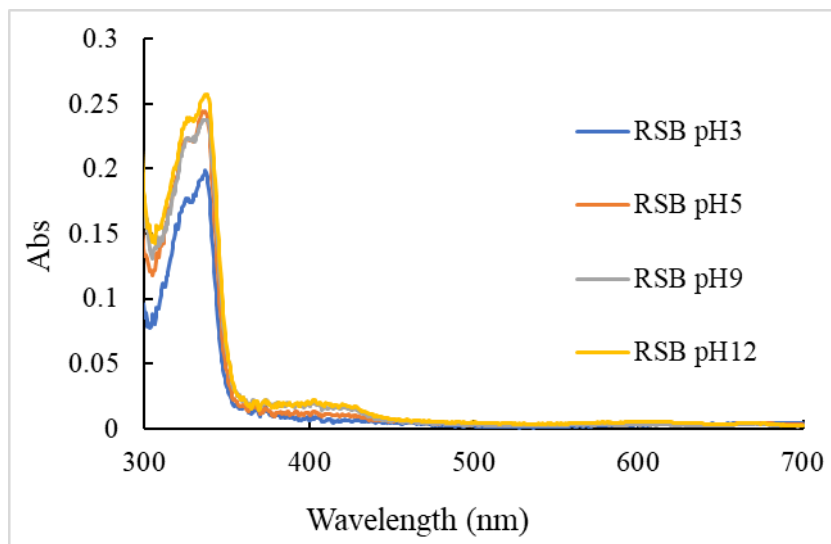


**Figure 7** Absorption spectra of  $1.00 \times 10^{-5}$  M of RSB at pH 3, 5, 9 and 12.

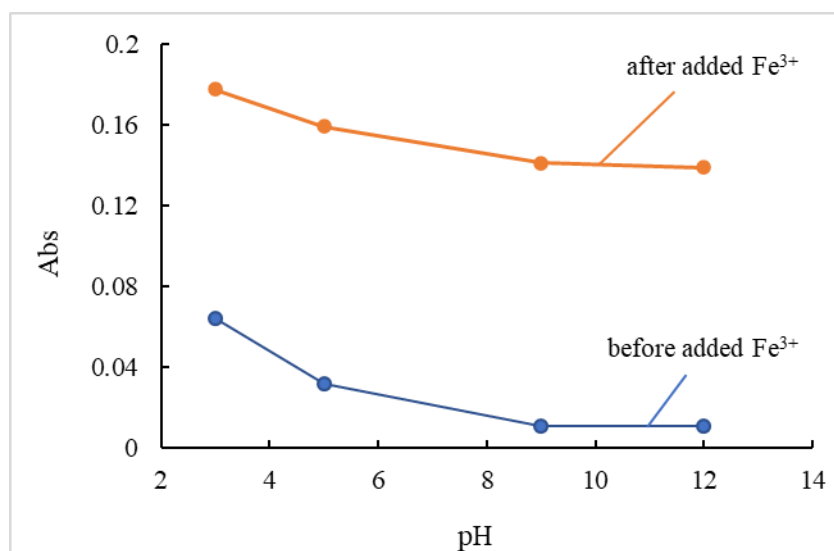


**Figure 8** The absorbance of  $1.00 \times 10^{-5}$  M of RSB before and after adding  $3.00 \times 10^{-4}$  M of  $Fe^{3+}$  solution at pH 3-12 measured at 380 nm.



The interference effects of various types of ions to the quantitative analysis were studied by analyzing  $\text{Fe}^{3+}$  solutions at a concentration level of  $1.00 \times 10^{-4}$  M, and the absorbance at 380 nm was determined. Then, other metal ions ( $3.00 \times 10^{-4}$  M) were added, and the absorbance was compared as shown in Figure 9. The results showed that the absorbance value when adding other metal ions changed by more than 5.00 %. Only  $\text{Fe}^{2+}$  had a change in absorbance of 12.94 %. However, determination of the amount of iron in water samples was the determination of the total amount of  $\text{Fe}^{3+}$  and  $\text{Fe}^{2+}$  and did not affect the analysis.

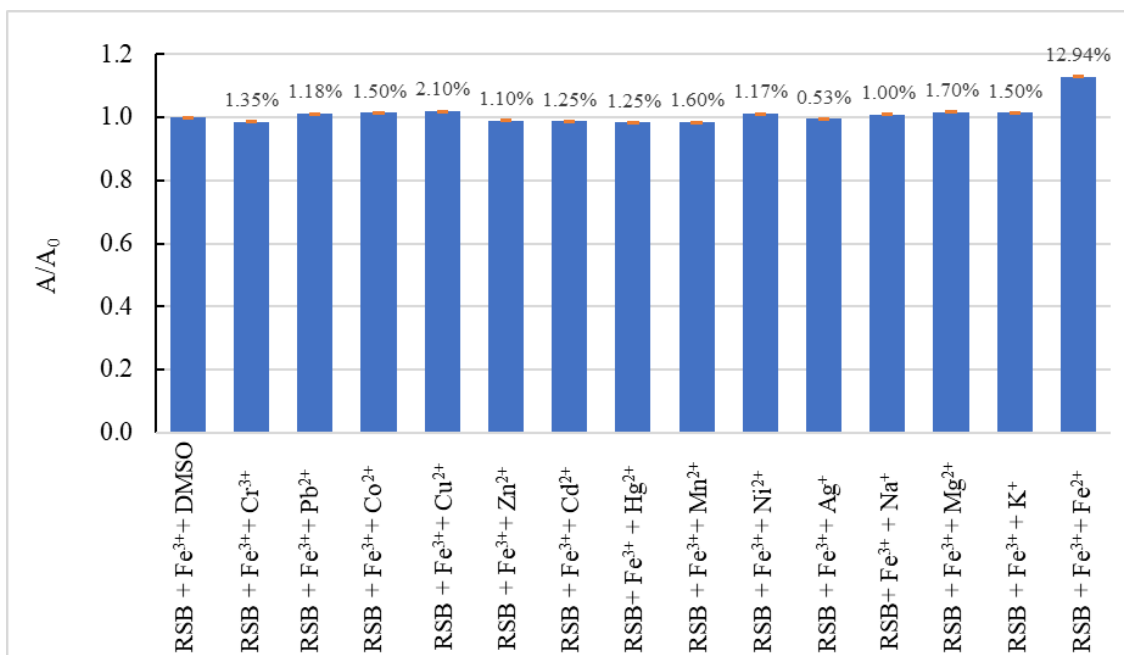


**Figure 9** The changes in absorbance at 380 nm of the 2.00 mL RSB ( $1.00 \times 10^{-5}$  M) mixed with 1.00 mL  $\text{Fe}^{3+}$  ( $1.00 \times 10^{-4}$  M) in the presence of different types of 1.00 mL cations ( $3.00 \times 10^{-4}$  M).

The reduced Schiff base ligand was applied as a sensor to quantify the amount of  $\text{Fe}^{3+}$  in real water samples from three sources; tap water, canal water and drinking water.  $\text{Fe}^{3+}$  solution with concentrations of  $1.00 \times 10^{-4}$  and  $3.00 \times 10^{-4}$  M were added to each water sample. Then, analysis was performed by mixing each type of water sample with reduced Schiff base ligand solution in a ratio of 1:1 by volume and the absorbance of the solutions was measured at 380 nm. The analysis results showed percentage recoveries ranging from 97.76% to 104.33%, with the measured  $\text{Fe}^{3+}$  concentrations differing from those obtained by the standard method only 1.51% to 2.70%, all within a 95% confidence interval, as shown in Table 1. The results indicated that the reduced Schiff base ligand was highly effective sensor for measuring the amount of  $\text{Fe}^{3+}$  in water samples, offering accuracy and reliability comparable to standard analytical methods.

**Table 1** Quantity of  $\text{Fe}^{3+}$  in real water samples using the developed method (reduced Schiff base ligand) comparison with the standard method, Inductive coupled plasma optical emission spectroscopy (ICP), and the percentage recovery from the developed method.

Type of sample	Spiked $[\text{Fe}^{3+}]$ (M)	$[\text{Fe}^{3+}]$ found (M) (RSD, n=3)		%Recovery (RSD, n=3)	%Error
		Reduced Schiff base	ICP		
Tap water	$1.00 \times 10^{-4}$	$0.99 \pm 0.160 \times 10^{-4}$ (1.62)	$1.01 \pm 0.007 \times 10^{-4}$ (0.70)	$98.80 \pm 1.60$	2.19
	$3.00 \times 10^{-4}$	$3.04 \pm 0.044 \times 10^{-4}$ (1.45)	$2.96 \pm 0.02 \times 10^{-4}$ (0.68)	$101.33 \pm 0.47$	2.70
Drinking water	$1.00 \times 10^{-4}$	$0.98 \pm 0.160 \times 10^{-4}$ (1.63)	$0.99 \pm 0.06 \times 10^{-4}$ (0.60)	$98.40 \pm 1.60$	1.28
	$3.00 \times 10^{-4}$	$3.13 \pm 0.046 \times 10^{-4}$ (1.47)	$3.05 \pm 0.025 \times 10^{-4}$ (0.82)	$104.33 \pm 1.47$	2.63
Canal water	$1.00 \times 10^{-4}$	$0.98 \pm 0.18 \times 10^{-4}$ (1.84)	$0.99 \pm 0.05 \times 10^{-4}$ (0.50)	$97.90 \pm 1.80$	1.51
	$3.00 \times 10^{-4}$	$2.93 \pm 0.018 \times 10^{-4}$ (0.61)	$2.87 \pm 0.015 \times 10^{-4}$ (0.52)	$97.76 \pm 0.60$	2.09

Comparing the results of the reduced Schiff base ligand with previous works on  $\text{Fe}^{3+}$  measurement showed that the reduced Schiff base ligand provided a wide measurement range and a lower LOD value than those obtained from many researches, as shown in Table 2. The measurement of 2-1000  $\mu\text{M}$  and LOD of 1.22  $\mu\text{M}$  were obtained from this study. Moreover, the developed method can be used to quantify  $\text{Fe}^{3+}$  in real water samples. Therefore, the reduced Schiff base ligand has potential as a sensor for detecting  $\text{Fe}^{3+}$  in natural water sources.

**Table 2** Comparison of efficiency of different sensors for detection of  $\text{Fe}^{3+}$

Type of probe	Mechanism	Linear range ( $\mu\text{M}$ )	LOD ( $\mu\text{M}$ )	References
Gold nanoparticles	Aggregation	10-60	5.60	[37]
Metal organic framework (MIL-53)	Ions exchange	3-200	9.00	[38]
Graphene quantum dots	Coordination	0-400	7.22	[39]
Silver nanoparticles	Reduction	0.08-80	0.08	[40]
Chromophore	Coordination	0-100	5.37	[41]
Silver nanoparticles	Coordination	9- 9000	7.90	[42]
Silver nanoparticles	Coordination	7-1790	1.79	[43]
Chromophore	Coordination	2-1000	1.22	This work

## Conclusions

The binding interaction between the reduced Schiff base ligand and  $\text{Fe}^{3+}$  was analyzed by UV-visible spectrophotometry. New peaks in the wavelength range of 350-400 nm were detected due to ligand-to-metal charge transfer (LMCT) upon complex formation. The absorbance of the complex at 380 nm has a linear correlation with the amount of added  $\text{Fe}^{3+}$ . In this study, the reduced Schiff base ligand can be applied as a sensor for analyzing the amount of  $\text{Fe}^{3+}$  in real water samples. The developed analytical method gave a linear standard curve in the concentration range from  $2.00 \times 10^{-6}$ – $1.00 \times 10^{-3}$  M with LOD and LOQ of  $1.22 \times 10^{-6}$  and  $2.03 \times 10^{-6}$  M, respectively. This method showed analytical results similar to those obtained from standard techniques. Therefore, this method offers a cost-effective, rapid, and straightforward approach for  $\text{Fe}^{3+}$  quantification in real water samples, requiring minimal reagent quantities.

## Acknowledgements

The authors would like to thank Faculty of Science, Srinakharinwirot University for the supporting research tools and facilities. Scholarship for student from the collaboration with Thailand International Cooperation Agency (TICA) is gradually acknowledged.

## References

1. Abbaspour N, Hurrell R, Kelishadi R. Review on iron and its importance for human health. *J Res Med Sci.* 2014;19(2):164-74.
2. Ali MK, Kim RY, Karim R, Mayall JR, Martin KL, Shahandeh A, et al. Role of iron in the pathogenesis of respiratory disease. *Int J Biochem Cell Biol.* 2017;88:181-95.
3. Cheng R, Dhorajia VV, Kim J, Kim Y. Mitochondrial iron metabolism and neurodegenerative diseases. *Neurotoxicology.* 2022;88:88-101.
4. Rishi G, Subramaniam VN. Biology of the iron efflux transporter, ferroportin. *Adv Protein Chem Struct Biol.* 2021;123:1-16.
5. Wu Q, Wei C, Guo S, Liu J, Xiao H, Wu S, et al. Acute iron overload aggravates blood-brain barrier disruption and hemorrhagic transformation after transient focal ischemia in rats with hyperglycemia. *IBRO Neurosci Rep.* 2022;13:87-95.
6. Baschant U, Altamura S, Steele-Perkins P, Muckenthaler MU, Spasić MV, Hofbauer LC, et al. Iron effects versus metabolic alterations in hereditary hemochromatosis driven bone loss. *Trends Endocrinol Metab.* 2022;33(9):652-63.
7. Liu S, Cao X, Wang D, Zhu H. Iron metabolism: state of the art in hypoxic cancer cell biology. *Arch Biochem Biophys.* 2022;723:109199.
8. Rishi G, Huang G, Subramaniam VN. Cancer: the role of iron and ferroptosis. *Int J Biochem Cell Biol.* 2021;141:106094.
9. Higashida K, Inoue S, Nakai N. Iron deficiency attenuates protein synthesis stimulated by branched-chain amino acids and insulin in myotubes. *Biochem Biophys Res Commun.* 2020;531(2):112-7.

10. Dai Y, Liu X, Wang P, Fu J, Yao K, Xu K. A new fluorescent probe based on quinoline for detection of  $Al^{3+}$  and  $Fe^{3+}$  with “off-on-off” response in aqueous solution. *RSC adv.* 2016;6(102):99933-9.
11. Wang L, Yang L, Cao D. A visual and fluorometric probe for Al(III) and Fe(III) using diketopyrrolopyrrole-based Schiff base. *Sens Actuators B: Chem.* 2014;202:949-58.
12. Freelandgraves JH, Sachdev PK, Binderberger AZ, Sosanya ME. Global diversity of dietary intakes and standards for zinc, iron, and copper. *J Trace Elem Med Biol.* 2020;61:126515.
13. Zachariou V, Bauer CE, Seago ER, Panayiotou G, Hall ED, Butterfield DA, et al. Healthy dietary intake moderates the effects of age on brain iron concentration and working memory performance. *Neurobiol Aging.* 2021;106:183-96.
14. Asmari M, Abdel-Megied AM, Michalcová L, Glatz Z, El Deeb S. Analytical approaches for the determination of deferiprone and its iron(III) complex: investigation of binding affinity based on liquid chromatography-mass spectrometry (LC-ESI/MS) and capillary electrophoresis-frontal analysis (CE/FA). *Microchem J.* 2020;154:104556.
15. Pattaweepaiboon S, Foytong W, Phiomphu N, Nanok T, Kaewchangwat N, Suttisintong K, et al. Spirooxazine-based dual-sensing probe for colorimetric detection of  $Cu^{2+}$  and  $Fe^{3+}$  and its application in drinking water and rice quality monitoring. *ACS omega.* 2022;7(22):18671-80.
16. Sun Y, Jia Y, Han W, Sun Y, Wang J, Deng Z, et al. A highly selective and sensitive coumarin-based chemosensor for recognition of  $Al^{3+}$  and the continuous identification of  $Fe^{3+}$  in water-bearing system and biomaging & biosensing in Zebrafish. *J Mol Struct.* 2023;1284:135459.
17. Zhang S, Liu C, Yuan Y, Fan M, Zhang D, Wang D, et al. Selective, highly efficient extraction of Cr(III), Pb(II) and Fe(III) from complex water environment with a tea residue derived porous gel adsorbent. *Bioresour Technol.* 2020;311:123520.
18. Chen G, Lan H, Cai S, Sun B, Li X, He Z, et al. Stable hydrazone-linked covalent organic frameworks containing O, N, O-chelating sites for Fe(III) detection in water. *ACS Appl Mat Interfaces.* 2019;11(13):12830-7.
19. Mohamed KN, Gledhill M. Determination of specific iron chelator by using LC-ICP-MS and LC-ESI-MS. *Procedia Environ Sci.* 2015;30:256-61.
20. Wu D, Sedgwick AC, Gunnlaugsson T, Akkaya EU, Yoon J, James TD. Fluorescent chemosensors: the past, present and future. *Chem Soc Rev.* 2017;46(23):7105-23.
21. Li W, Wang L, Tang H, Cao D. Diketopyrrolopyrrole-based fluorescent probes for detection and bioimaging: current progresses and perspectives. *Dyes Pigm.* 2019;162:934-50.
22. Balamurugan R, Liu J, Liu B. A review of recent developments in fluorescent sensors for the selective detection of palladium ions. *Coord Chem Rev.* 2018;376:196-224.
23. Gupta VK, Singh AK, Kumawat LK. Thiazole Schiff base turn-on fluorescent chemosensor for  $Al^{3+}$  ion. *Sens Actuators B: Chem.* 2014;195:98-108.
24. Gupta VK, Singh AK, Kumawat LK. A turn-on fluorescent chemosensor for  $Zn^{2+}$  ions based on antipyrine schiff base. *Sens Actuators B: Chem.* 2014;204:507-14.
25. Fang H, Huang P, Wu F. A highly sensitive fluorescent probe with different responses to  $Cu^{2+}$  and  $Zn^{2+}$ . *Spectrochim Acta A: Mol Biomol Spectrosc.* 2019;214:233-8.

26. Song H, Zhang Z. A quinoline-based ratiometric fluorescent probe for discriminative detection of  $Zn^{2+}$  and  $Cd^{2+}$  with different binding modes, and its  $Zn^{2+}$  complex for relay sensing of pyrophosphate and adenosine triphosphate. *Dyes Pigm.* 2019;165:172-81.
27. Mironenko AY, Tutov M, Chepak A, Zadorozhny P, Bratskaya SY. A novel rhodamine-based turn-on probe for fluorescent detection of  $Au^{3+}$  and colorimetric detection of  $Cu^{2+}$ . *Tetrahedron.* 2019;75(11):1492-6.
28. Li Y, Niu Q, Wei T, Li T. Novel thiophene-based colorimetric and fluorescent turn-on sensor for highly sensitive and selective simultaneous detection of  $Al^{3+}$  and  $Zn^{2+}$  in water and food samples and its application in bioimaging. *Anal Chim Acta.* 2019;1049:196-212.
29. Zhang M, Gong L, Sun C, Li W, Chang Z, Qi D. A new fluorescent-colorimetric chemosensor based on a Schiff base for detecting  $Cr^{3+}$ ,  $Cu^{2+}$ ,  $Fe^{3+}$  and  $Al^{3+}$  ions. *Spectrochim Acta A: Mol Biomol Spectrosc.* 2019;214:7-13.
30. Liu J, Zheng Q, Yang J, Chen C, Huang Z. A new fluorescent chemosensor for  $Fe^{3+}$  and  $Cu^{2+}$  based on calix [4] arene. *Tetrahedron Lett.* 2002;43(50):9209-12.
31. Li N, Xu Q, Xia X, Lu J, Wen X. A polymeric chemosensor for  $Fe^{3+}$  based on fluorescence quenching of polymer with quinoline derivative in the side chain. *Materials Chemistry and Physics.* 2009;114(1):339-43.
32. Li Z, Zhang L, Zhao W, Li X, Guo Y, Yu M, et al. Fluoranthene-based pyridine as fluorescent chemosensor for  $Fe^{3+}$ . *Inorganic Chem Comm.* 2011;14(10):1656-8.
33. Li Z, Zhou Y, Yin K, Yu Z, Li Y, Ren J. A new fluorescence “turn-on” type chemosensor for  $Fe^{3+}$  based on naphthalimide and coumarin. *Dyes Pigm.* 2014;105:7-11.
34. Wang R, Wan Q, Feng F, Bai Y. A novel coumarin-based fluorescence chemosensor for  $Fe^{3+}$ . *Chem Res Chin Univ.* 2014;30(4):560-5.
35. Aussawaponpaisan P, Nusuwan P, Tongraung P, Jittangprasert P, Pumsa-ard K, Kuno M. Fluorescent Chemosensor for  $Cu^{2+}$  based on Schiff base-naphthalene-2-ol. *Mater Today: Proc.* 2017;4(5):6022-30.
36. Sungwienwong I, Tongraung P, Boonsri P, Apiratikul N. Reduced Schiff base as novel two-faced sensor for the detection of iron (III) and carbonate ions. *J Mol Struct.* 2024;1308:138126.
37. Wu S, Chen Y, Sung Y. Colorimetric detection of  $Fe^{3+}$  ions using pyrophosphate functionalized gold nanoparticles. *Analyst.* 2011;136(9):1887-91.
38. Yang C, Ren H, Yan X. Fluorescent metal-organic framework MIL-53 (Al) for highly selective and sensitive detection of  $Fe^{3+}$  in aqueous solution. *Anal Chem.* 2013;85(15):7441-6.
39. Ananthanarayanan A, Wang X, Routh P, Sana B, Lim S, Kim D, et al. Facile synthesis of graphene quantum dots from 3D graphene and their application for  $Fe^{3+}$  sensing. *Adv Funct Mater.* 2014;24(20):3021-6.
40. Gao X, Lu Y, He S, Li X, Chen W. Colorimetric detection of iron ions (III) based on the highly sensitive plasmonic response of the N-acetyl-L-cysteine-stabilized silver nanoparticles. *Anal Chim Acta.* 2015;879:118-25.
41. Liu X, Li N, Xu M-M, Wang J, Jiang C, Song G, et al. Specific colorimetric detection of  $Fe^{3+}$  ions in aqueous solution by squaraine-based chemosensor. *RSC adv.* 2018;8(61):34860-6.

42. Samerjai W, Jittangprasert P, Tongraung P. Colorimetric detection of iron (III) ion based on 4-aminothiophenol and schiff base naphthalene-2-ol modified silver nanoparticles. *Asian J Chem.* 2020;32(2):287-92.
43. Jittangprasert. P, Kerdkok D, Tongraung, P. Synthesis and application of novel modified silver nanoparticles for determination of iron (III) in wastewater. *J Res Unit Sci Tech Environ Learning.* 2020;11(2):316-31. (in Thai)